SSCL-N-867

SSCL-N-867
July 1994
Distribution Category: 400

M. Levin

Low Temperature Test Results for the ASST Run 3

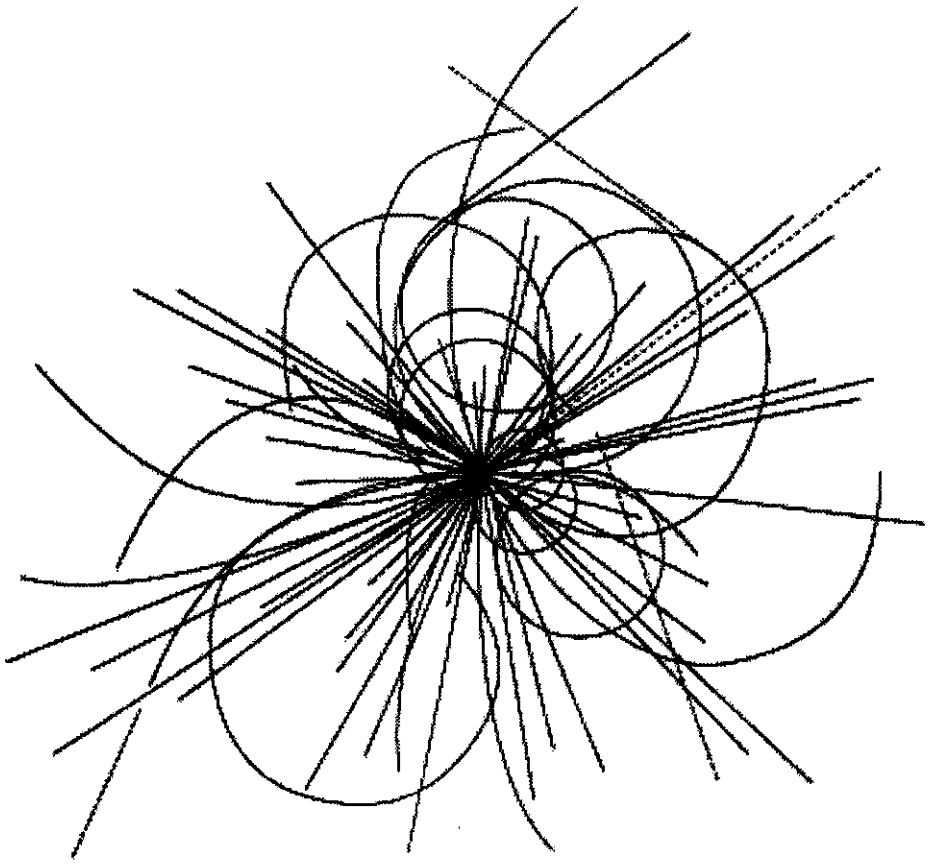

Superconducting Super Collider Laboratory

SSCL-N-867

Low Temperature Test Results for the ASST Run 3

M. Levin

Superconducting Super Collider Laboratory*
2550 Beckleymeade Ave.
Dallas, TX 75237

July 1994

*Operated by the Universities Research Association, Inc., for the U.S. Department of Energy under Contract No. DE-AC35-89ER40486.

1.0 INTRODUCTION

The string consists of two half cells with a recooler spool piece (SPR) in the middle. Each half cell consists of five full-length 50-mm aperture dipoles and one full-length quadrupole. The string configuration is: DCA313, DCA314, DCA315, DCA323, DCA322, QCC406, SPR, DCA316, DCA319, DCA320, DCA210, DCA212, and QCC405. The feed spool and end spool are at the ends of the string.

Figure 1 shows the arrangement of sensors used in the Accelerator Systems String Test (ASST) thermal measurements. At the lead end of each magnet's cold mass is a carbon glass thermometer with an accuracy of about 3 mK. The manufacturer of these sensors, Lake Shore Cryotronics, guarantees an accuracy of 5 mK, but these sensors were calibrated simultaneously resulting in the greater accuracy. However, accuracy changes with time becoming less reliable as the number of cooldown/warmup cycles increases. Vapor pressure thermometers (VPT) were installed in domes of the feed can and end can. The 20-K cooling line contains germanium resistance thermometers with an accuracy of 15 mK at the inlet and outlet of each magnet. Platinum resistance thermometers with an accuracy of 0.5 K are located on the 80-K shield cooling line. Resistive heaters are installed in the cold mass and in the 20-K circuits of each dipole so that a known amount of heat may be introduced into the dipole as part of a heat leak measuring technique. Warm pressure transducers are placed in each of the cryogenic pipes at the feed and end spools to determine the inlet and outlet conditions of the cryogenic flows. The single phase flow rate is measured with an in-line Venturi meter. The 20-K and 80-K shield flows are measured with room-temperature gas meters with an accuracy of about 0.5% (according to the manufacturer, American Meter).

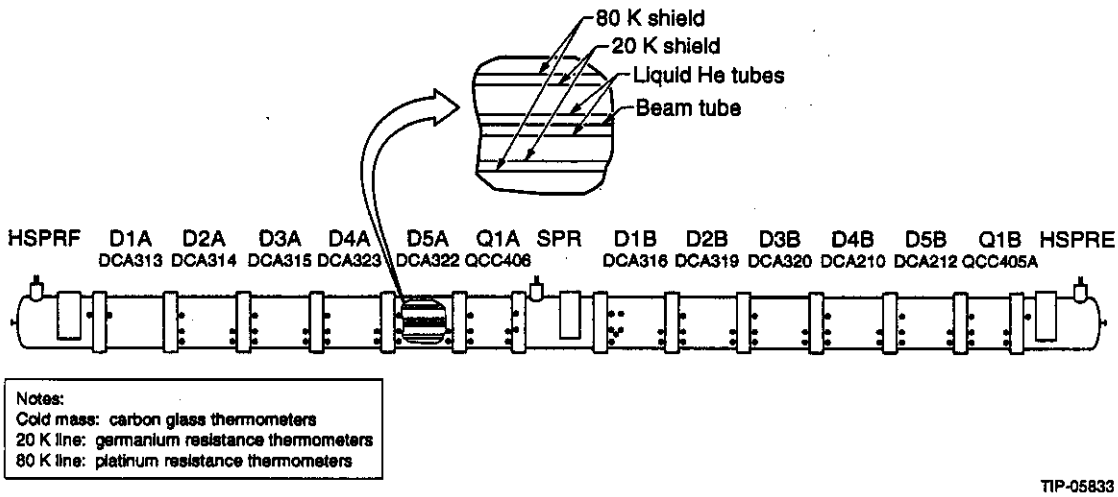

Figure 1. Arrangement of Sensors Used in ASST Thermal Measurements.

A few sensors did not work properly during heat leak measurements—the carbon glass resistors in the cold mass of dipoles 313, 323, 316, 212, and both quadrupoles; and the 20-K line germanium resistors in the return end of dipole 314 and in the lead ends of dipoles 315 and 323.

Sensors at the lead ends of dipoles 313 and 316 (the first dipoles of each half cell) performed satisfactorily but due to significant effect from the feed can and SPR they showed temperatures higher than at other dipoles. The explanation may be that the helium was not mixed enough causing the sensors to show higher temperatures than the average of the stream. Moreover, at the lead end of D316 four sensors were installed that were previously calibrated simultaneously. Each showed a temperature higher than shown by sensors in the next two dipoles, and different from

any of the other three. In addition, helium flows from one element of the string to another through two passages. One passage contains the power bus that limits helium flow through it, so that flow rates differ between the two. As a result, in locations where end effects are significant the temperature of these two flows also differs. There is not enough space in the dome of the dipole for complete mixing of helium, so sensors in this locations do not show the true average temperature of the flow. Besides that, carbon glass resistors are too small to integrate the temperature of flow across the cross-section, measuring instead the local temperature (at a point) rather than an average temperature of the flow. It may be concluded that the sensor installation technique must be designed very carefully with all possible precautions for obtaining correct data in order to be useful in so complex and expensive test facilities as the ASST.

The carbon glass resistor at the lead end of DCA323 was dead and the average of the values from two TVO (Russian carbon resistor) sensors installed on the external surface of helium tubes within the magnet interconnect was used for heat leak calculations. The temperature difference between internal and external sensors was estimated to be about 40 mK.

Sensors in both quadrupoles were installed without noting their serial numbers, and their calibration functions were therefore unknown. Fortunately, two more TVO sensors had been installed on the external surface of the helium piping between QCC406 and SPR. One of them failed during closing of the interconnection but the other was used successfully for heat leak measurements.

The sensor at the lead end of DCA323 in the 20-K line was dead. Sensors at the return end of DCA314 and the lead end of DCA315 showed temperatures in reverse order, with the upstream sensor showing a higher value than the downstream sensor and a difference of about 40 mK. This was attributed to a calibration problem and for heat leak calculations their average value was used.

To measure heat leak, the system was allowed to come to thermal equilibrium prior to measuring the inlet and outlet temperatures as well as flow rates and pressures of the helium flowing through the cold mass and 20-K line. The heat leak was calculated by the energy balance equation:

$$Q = G*(h2 - h1),$$

where: Q = heat leak;

G = the mass flow rate of helium;

h1 and h2 = enthalpies of the helium at the inlet and outlet points of the magnets.

For the 80-K line it was not possible to obtain steady-state conditions required for heat leak measurements because it was necessary to refill the nitrogen gas generator approximately every 10 hours. The frequent refilling did not leave sufficient time to achieve equilibrium in the 80-K shield so no heat leak measurements were made during Run #3.

2.0 COLD MASS

Heat leak measurements under a variety of conditions yielded the following results:

Flow rate (g/s)	Temperature of the 20-K shield (K)	Average heat leak (W)
~ 47	20–27	1.25
~ 47	28–34	1.55
~ 46	44–48	2.05
~ 23	45–49	2.22
~ 18	48–52	2.47

Details are presented in Table 1. There were not enough sensors in half-cell B for reliable measurements. Measurements at half cell A showed essentially the same average heat leak as obtained during Runs 1 and 2 (~1.3 W when the 20-K shield is about 20 K), confirming the reliability of the data. Accuracy of measurement was calculated by comparing the temperature rise across the middle three dipoles with the absolute accuracy of the temperature sensors—about 30%. The average heat leak was determined from the total heat leak for the middle three dipoles divided by 3. The heat leak average was used in order to reduce measurement error. It's important to realize the difficulty of measuring heat leak for only one dipole. The heat load budget of 0.36 W when the flow is 50 g/s presupposes the temperature difference less than 2 mK. Accuracy of the sensors used was about 3–5 mK (in the best case), so measurement of a single dipole would not be closer than 250% (or worse). During Run 3 some measurements were done under special conditions requested by the Magnet Division for purposes of verifying results reported from a mathematical model of the string: the temperature of the 20-K shield was higher than operational and the flow rate was reduced. The heat leak to the cold mass under these conditions was higher, as expected.

Two heater tests were done during Run 3. A known amount of heat was introduced into the helium and this was compared to the additional heat measured by the increase of the temperature rise across the string. The additional heat was put into a third dipole, DCA315. The first test showed the difference between thermally measured and electrically measured amounts of additional heat to be about 4%, due primarily to instability of the flow rate and also to inaccuracy of the temperature measurements. The second test was not completed. There were two heater tests during Run #2 as well, producing differences of 4% and 6%.

3.0 20-K LINE

The results of heat leak measurements are presented in Table 2. The heat leaks found during Run 3 were in the same range as those found during Run 2, and close to the budget (5.06 W); with the exception that in each half cell, the fourth dipole—DCA323 and DCA210, specifically, showed higher heat leaks. The reason for that is not clear, but some ideas will be offered in the section about interconnect region measurements below. Unfortunately it was impossible to check for thermal short circuits between the 20-K/80-K shields by measurement of heat leaks to the 80-K shield. The heater test showed that the flow instability gives rise to about a 10% accuracy in the flow rate measurement. The temperature of the 80-K shield during these measurements was about 82 K.

The end effects are seen in this experiment were significant as in previous runs. The same effect was observed around SPR. Some descriptions of existing end effects were presented in previous publications and are not repeated here.

Tables 3 and 4 give some idea of the stability of conditions during thermal measurements.

4.0 THERMAL SHIELDS

An attempt to determine the temperature distribution across the temperature shields and the effectiveness of contact between different parts of each shield (interconnect and cryostat) was made during Run #3. Since it is important to know the temperature difference between the cooling flow and the temperature of the shield itself, additional sensors were installed on the 20-K and 80-K shields in two interconnect regions around DCA323. The TVO-type carbon resistors were installed on the 20-K shields and platinum resistors were installed on the 80-K shields. Sixteen sensors were installed: four on each shield in each location (see Figure 2), as follows: two sensors were installed on each shield very close to the cooling pipe, one on the cryostat shield and one on

the interconnect shield. Two sensors were installed on the diametrically opposite side of each shield, one on the cryostat shield and one on the interconnect shield (see Figures 3 and 4).

The platinum resistors are screw-shaped for easy installation and they were used for the 80-K shield. A special method was developed for installation of carbon resistors on the 20-K shield, as follows: Since TVO sensors are ordinary radio resistors, special elements are required to ensure good thermal contact between the sensor and the shield. Therefore, small aluminum boxes (1.5 × 1.5 × 1 cm) were welded to the shields and the carbon resistors were put in special holes in these boxes with thermal conducting grease.

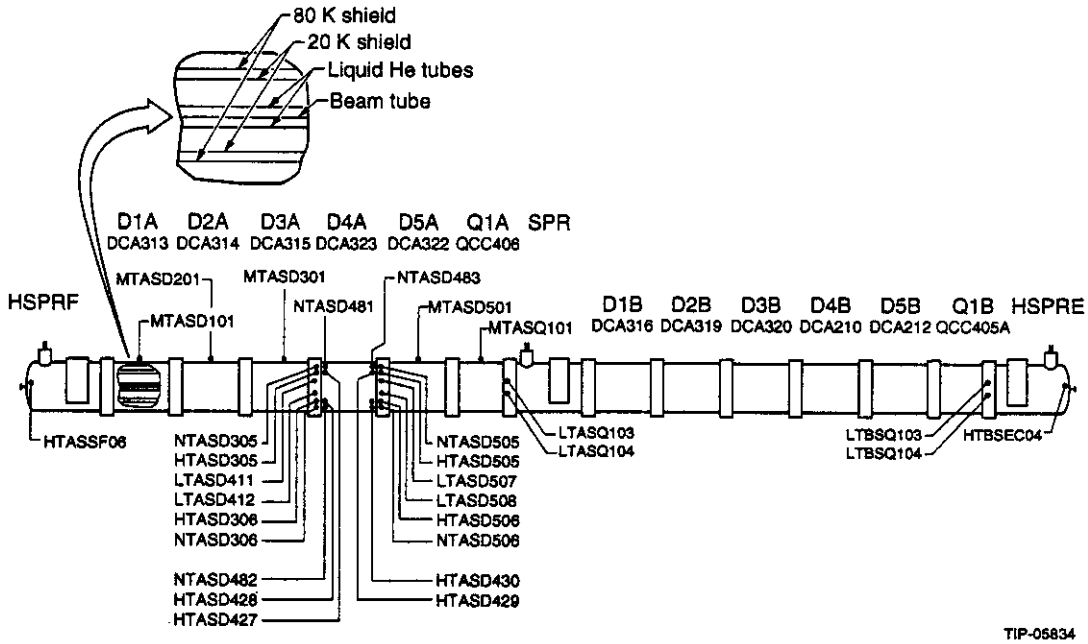

Figure 2. Arrangement of Thermal Shield Sensors.

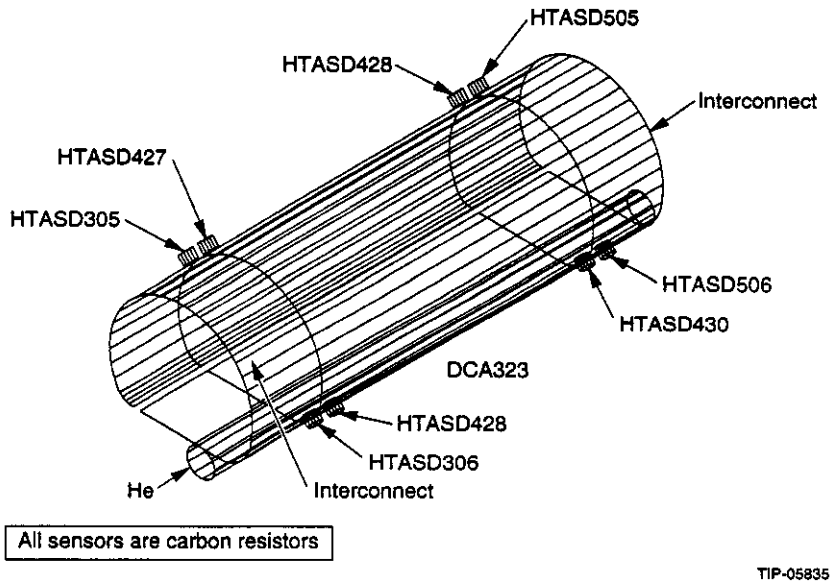

Figure 3. 20-K Shield Temperature Sensor Location.

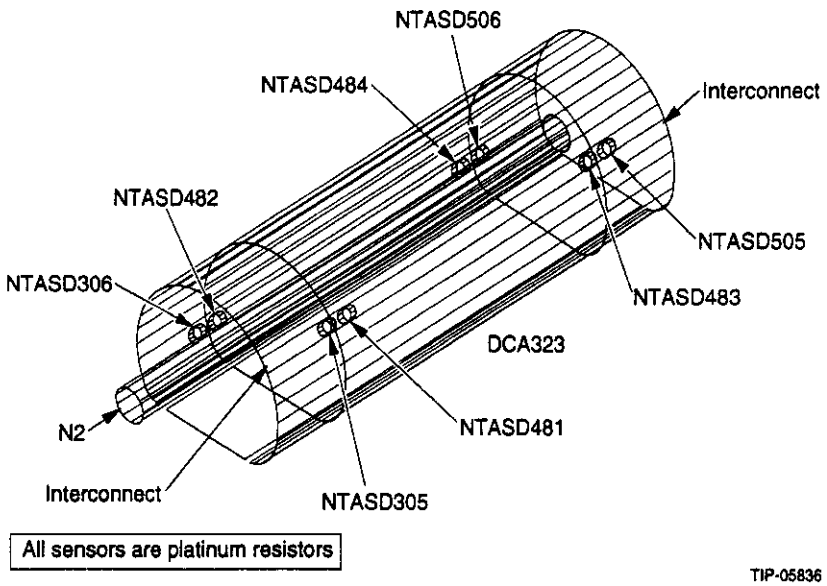

Figure 4. 80-K Shield Temperature Sensor Location.

4.1 20-K Shield

The 20-K shield in the region of DCA323 was tested at different temperatures: ~25 K, ~30 K, ~45 K. Data are presented in Table 5.

4.1.1 Interconnection DCA315–DCA323

Sensor HTASD428 was broken during installation and could not be repaired. Other sensors at this location showed temperatures to be in expected order: the closer to the cooling pipe, the lower the temperature.

The temperature difference between the cooling flow and the 20-K shield was about 1 K, a little higher than expected.

The temperature difference across the shield was about 0.2–0.3 K, and the difference between the magnet's shield and the interconnect's shield shown by the upper sensors was about 0.1 K.

It is important to note that the interconnect's shield is not fixed to the cooling pipe.

4.1.2 Interconnection DCA323–DCA322

The temperature difference between cooling flow and shield was also about 1 K. The temperature difference across the shield was about 0.3–0.5 K at the magnet's shield and 0–0.1 K at the interconnect's shield. The cause of this is not known, but it is unlikely that it was due to sensors calibration error.

4.2 80-K Shield

The interconnect shield is not fixed to the cooling pipe. Data are presented in Table 5.

4.2.1 Interconnection DCA315–DCA323

Temperatures in both parts of the shield (magnet and interconnect) nearest to the cooling pipe location (lower side on the schematic) were about 8 K higher than the temperature of the cooling flow, indicating the possibility of thermal contacts with the cryostat. The upper temperature sensors showed temperatures about 2 K lower than the lower side sensors, and that could only be due to thermal contacts between 80-K and 20-K shields somewhere inside the cryostat.

4.2.2 Interconnection DCA323–DCA322

The situation here was almost the same as for DCA315-DCA323 interconnection, with the exception that the temperature difference between the cooling flow and the magnet's shield near the cooling pipe was higher than 10 K. At the same time, the temperature difference between the cooling flow and the interconnect's shield was about 5 K. This also may indicate thermal contacts with the cryostat.

5.0 CONCLUSIONS

The measurement technique used in heat leak experiments provided repeatable results during all three experimental runs of the ASST. The measurement of the cold mass heat leak was the most difficult and was the least accurate. The accuracy could be increased by using vapor pressure thermometers and special installation technique for integration of the flow temperature. Besides that, replacing the SPR with the dipole could provide the best possible string configuration for precise heat leak measurements.

Table 1. Heat Leak Measurements, Cold Mass (Run 3).

Date	Start Time+ Duration	Flow Rate g/s	D1 W	D2 W	D3 W	D4 W	D5+Q1 W	heater W	dQ heater %	20 K In. K	(2+3+4)/3 W
cell A											
09-29-93	9:00+2.0	46.10	5.110	1.110	(D3+D4)=2.44					20–24	1.19
09-30-93	2:00+8.0	47.63	4.820	1.381	(D3+D4)=2.524					22–27	1.30
10-06-93	1:30+5.5	47.37	8.906	1.800	1.611	1.137	18.710			28–33	1.52
10-07-93	0:00+7.0	47.26	8.696	2.269	"H" 4.537	0.662	17.913	2.776	~4	29–34	1.56
10-07-93	17:00+4.0	47.22	8.829	1.794	1.794	1.133	17.422			21–27	1.57
10-09-93	17:00+3.0	45.93	4.820	2.530	1.650	1.970	19.110			44–48	2.05
10-12-93	21:00+1.7	17.84	12.130	1.873	"H" 6.903	1.427		2.776		48–52	2.47
10-17-93	10:00+6.0	22.94	5.740	2.680	2.570	1.420	11.900			45–49	2.22
cell B											
10-06-93	1:30+5.5	47.37		14.590	6.870		D2+D3+D4+D5+Q= 33.54			28–33	
10-07-93	0:00+7.0	47.26		15.880	"H" 7.042		D2+D3+D4+D5+Q= 32.1		~25	29–34	
10-07-93	17:00+4.0	47.22		14.684	6.799		D2+D3+D4+D5+Q= 33.48			21–27	
10-09-93	17:00+3.0	45.93		14.970	7.260		D2+D3+D4+D5+Q= 35.23			44–48	
10-17-93	10:00+6.0	22.94		3.190	1.310		D2+D3+D4+D5+Q= 24.68			45–49	
				H" means the internal heater turned ON							

Table 2. Heat Leak Measurements, 20-K Shield.

Date	Start Time+ Duration	Flow Rate g/s	D1 W	D2 W	D3 W	D4 W	D5+Q1 W	heater W	dQ heater %	(2+3+4+5)/4
cell A										
10-06-93	12:00+3:00	1.75	8.36	4.62	5.25	~8.8	5.016+6.76			5.92
10-07-93	14:20+18	1.69	8.35	4.45	4.84	"H"	5.021+6.55	5.00	~4	6.19
10-08-93	9:30+3	1.69	9.88	5.87	6.11	~9.7	5.567+6.804			6.96
cell B										
10-06-93	12:00+3:00	1.75	6.06	5.69	6.08	6.82	9.05+13.85			7.62
10-07-93	14:20+18	1.69	6.04	5.68	6.03	"H"	8.61+13.41	4.99	~10	7.79
10-08-93	9:30+3	1.69	6.47	5.95	6.22	7.10	8.97+13.26			7.78
			H" means the internal heater turned ON							

Table 3. Temperature Distribution Along the String During Heat Leak Measurements, Cold Mass.

date/ start time+ duration		flow rate g/s	VPT FC K	AD201 K	AD301 K	AD411 K	AD412 K	AD501 K	AQ103 K	BD201 K	BD301 K	BD401 K	VPT EC K
10-06-93	Min	43.733	4.593	4.630	4.638	4.647	4.644	4.650	4.730	4.808	4.872	4.902	4.956
1:30+5.5	Max	52.031	4.601	4.642	4.647	4.657	4.653	4.660	4.743	4.819	4.881	4.910	4.964
	Mean	47.368	4.596	4.635	4.643	4.651	4.648	4.655	4.737	4.812	4.879	4.906	4.959
10-07-93	Min	43.270	4.602	4.640	4.650	4.675	4.663	4.673	4.751	4.819	4.885	4.916	4.976
00:00+7	Max	51.749	4.606	4.645	4.655	4.681	4.670	4.679	4.759	4.826	4.895	4.927	4.982
	Mean	47.263	4.604	4.643	4.653	4.678	4.667	4.676	4.755	4.822	4.892	4.923	4.979
10-07-93	Min	43.817	4.601	4.639	4.648	4.657	4.653	4.660	4.735	4.780	4.845	4.875	4.927
17:00+4	Max	52.565	4.604	4.643	4.651	4.660	4.657	4.664	4.742	4.785	4.849	4.878	4.931
	Mean	47.515	4.602	4.641	4.649	4.658	4.655	4.662	4.739	4.782	4.847	4.877	4.930
10-09-93	Min	42.076	4.141	4.169	4.185	4.202	4.187	4.205	4.320	4.726	4.794	4.828	4.884
17:00+3	Max	48.590	4.148	4.177	4.192	4.209	4.195	4.214	4.330	4.732	4.801	4.834	4.900
	Mean	45.928	4.144	4.173	4.188	4.205	4.190	4.210	4.325	4.730	4.798	4.831	4.890
10-12-93	Min	15.936	4.093	4.288	4.320	4.470	4.378	4.447	5.382	5.122	5.132	5.202	5.302
21:00+~2	Max	19.378	4.124	4.304	4.333	4.489	4.386	4.462	5.398	5.147	5.153	5.251	5.328
	Mean	17.838	4.108	4.296	4.325	4.481	4.382	4.454	5.392	5.132	5.140	5.228	5.314
10-17-93	Min	21.485	3.895	3.982	4.019	4.070	4.030	4.067	5.197	4.849	4.879	4.891	5.059
10:00+6	Max	24.356	3.897	3.984	4.020			4.068	5.203	4.856	4.884	4.896	5.064
	Mean	22.943	3.896	3.983	4.019			4.067	5.200	4.852	4.881	4.893	5.062

Table 4. Temperature Distribution Along the String During Heat Leak Measurements, 20-K Line.

A CELL														
date/ start time+ duration		flow rate g/s	AD101 K	AD103 K	AD201 K	AD203 K	AD301 K	AD303 K	AD401 K	AD403 K	AD501 K	AD503 K	AQ101 K	AQ103 K
10-06-93	Min		33.18	32.25	32.00	31.54	31.59	31.01			29.98	29.47	29.33	28.56
12:00+3	Max		33.52	32.62	32.58	32.00	31.99	31.43			30.53	29.93	29.82	29.18
	Mean	1.75	33.32	32.41	32.28	31.74	31.78	31.20			30.24	29.70	29.59	28.85
10-07-93	Min		34.58	33.61	33.39	32.95	33.02	32.35		30.69	30.58	30.11	29.95	29.16
14:20+18	Max		35.24	34.33	34.35	33.63	33.67	33.10		31.47	31.34	30.80	30.68	30.05
	Mean	1.69	34.90	33.95	33.78	33.26	33.30	32.73		31.03	30.98	30.41	30.30	29.56
10-08-93	Min		34.21	33.15	32.92	32.30	32.37	31.72		30.63	30.55	29.94	29.85	29.04
9:30+2.5	Max		34.93	33.77	33.74	32.94	32.96	32.14		31.01	30.91	30.28	30.17	29.42
	Mean	1.69	34.54	33.42	33.26	32.58	32.61	31.91		30.80	30.74	30.11	30.00	29.23
B CELL														
date/ start time+ duration		flow rate g/s	BD101 K	BD103 K	BD201 K	BD203 K	BD301 K	BD303 K	BD401 K	BD403 K	BD501 K	BD503 K	BQ101 K	BQ103 K
10-06-93	Min		26.41	25.75	25.59	24.97	24.87	24.21	24.10	23.38	23.28	22.33	22.32	20.73
12:00+3	Max		26.85	26.17	26.02	25.41	25.30	24.65	24.54	23.81	23.70	22.67	22.68	21.20
	Mean	1.75	26.63	25.97	25.82	25.20	25.10	24.44	24.33	23.58	23.48	22.50	22.50	20.99
10-07-93	Min		26.90	26.19	26.03	25.35	25.24	24.51	24.39	22.82	22.73	21.75	21.72	20.15
14:20+18	Max		27.59	26.91	26.77	26.14	26.02	25.36	25.26	23.81	23.70	22.70	22.73	21.28
	Mean	1.69	27.24	26.56	26.41	25.77	25.66	24.98	24.87	23.40	23.30	22.33	22.32	20.81
10-08-93	Min		26.76	26.04	25.89	25.22	25.11	24.41	24.29	23.49	23.38	22.38	22.37	20.85
9:30+2.5	Max		26.90	26.12	25.95	25.29	25.18	24.51	24.40	23.59	23.49	22.46	22.45	21.00
	Mean	1.69	26.81	26.08	25.93	25.25	25.15	24.45	24.33	23.53	23.43	22.42	22.41	20.91

Table 5. Shield Temperatures, 20-K Shield.

20-K Shield											
Date	**Start Time+ Duration**	**HT401**	**HT428**	**HT306**	**HT427**	**HT305**	**HT403**	**HT430**	**HT506**	**HT429**	**HT505**
09-30-93	2:00+8.0	25.88		27.00	27.32	27.42	25.37	26.18	26.34	26.72	26.46
10-06-93	1:30+5.5	31.20		32.25	32.47	32.59	30.24	31.31	31.78	31.68	31.35
10-07-93	0:00+7.0	32.19		32.44	32.70	32.82	30.51	31.37	31.46	31.78	31.45
10-07-93	17:00+4.0	32.73		33.47	33.70	33.82	31.03	31.89	32.02	32.42	32.07
10-08-93	9:30+3.0	31.91		32.86	33.13	33.25	30.80	31.72	31.82	32.14	31.81
10-09-93	17:00+3.0	46.05		46.81	47.05	47.13	45.46	46.10	46.04	46.23	45.70
10-17-93	10:00+6.0	47.07		47.76	47.96	48.03	46.45	47.10	47.04	47.23	46.69
80-K Shield											
Date	**Start Time+ Duration**	**NT401**	**NT482**	**NT306**	**NT481**	**NT305**	**NT403**	**NT484**	**NT506**	**NT483**	**NT505**
09-30-93	2:00+8.0	82.00	90.16	89.08	86.86	87.06	82.00	94.76	88.12	86.27	87.21
10-06-93	1:30+5.5	81.–84.	91.34	90.31	88.09	88.29	81.–84.	95.96	89.48	87.52	88.37
10-07-93	0:00+7.0	81.–84.	90.64	89.79	87.58	87.81	81.–84.	95.35	88.73	86.96	87.82
10-07-93	17:00+4.0	80.5–84.	90.63	89.85	87.65	87.87	80.5–84.	95.44	88.77	87.05	87.91
10-08-93	9:30+3.0	80.–84	90.22	89.42	87.18	87.44	80.–84	94.97	88.30	86.55	87.38
10-09-93	17:00+3.0	81.–84.	89.98	89.43	87.18	87.43	81.–84.	94.80	88.19	86.40	87.23
10-17-93	10:00+6.0	81.5–82.5	89.96	89.19	86.94	87.17	81.5–82.5	94.71	88.09	86.23	87.08
10-08-93	9:30+3.0	80.–84	90.22	89.42	87.18	87.44	80.–84	94.97	88.30	86.55	87.38

ACKNOWLEDGMENTS

The string test was operated under the guidance of P. Kraushaar, A. McInturff and G. Mulholland with the technical support of M. Hentges and their staff.

LIST OF PUBLICATIONS ABOUT ASST

1. "Full-Power Test of a String of Magnets Comprising a Half-Cell of the Superconducting Super Collider," SSCL-Preprint-162, Oct. 1992., 50 pp., *Particle Accelerators*, Vol. **43**, 1993.

2. "Cryogenic and Power Testing of a String of 50-mm Aperture Dipole Magnets at the Superconducting Super Collider Laboratory," *Proceedings of the XV International Conference on High Energy Accelerators*, Hamburg, Germany, July 1992, *International Journal of Modern Physics A*, **2B**, p. 671 (1993)

3. "Half Cell Operations Tests of the Superconducting Super Collider Laboratory," *IEEE Transactions on Applied Superconductivity*, Vol. **3**, No. 1, p. 622 (1993)

4. "Cryogenic Characteristics of the SSC Accelerator Systems String Test (ASST)," SSCL-Preprint-251, Apr. 1993, 4 pp., *Proceedings of the Fifth IISSC*, San Francisco, CA (1993).

5. "Collider Scenario Implications of ASST Operations," SSCL-Preprint-434, May 1993, 3 pp., *Proceedings of the 1993 Particle Accelerator Conference (PAC 93)*, Washington, DC, May 1993.

6. "Heat Leak Performance of SSC Collider Dipole Magnets," SSCL-Preprint-508, Sept. 1993, *Proceedings of the 13th International Conference on Magnet Technology*, Victoria, British Columbia, September 1993.